Reduction of PPP convergence period through pseudorange multipath and noise mitigation

Garrett Seepersad & Sunil Bisnath

GPS Solutions
The Journal of Global Navigation Satellite Systems

ISSN 1080-5370

GPS Solut
DOI 10.1007/s10291-014-0395-3

Springer

GPS Solut
DOI 10.1007/s10291-014-0395-3

ORIGINAL ARTICLE

Reduction of PPP convergence period through pseudorange multipath and noise mitigation

Garrett Seepersad · Sunil Bisnath

Received: 15 November 2013 / Accepted: 25 June 2014

Abstract Pseudorange multipath and pseudorange noise are the largest remaining unmanaged error sources in PPP. It is proposed that by reducing the effects of multipath and noise on the pseudorange observable, accurate estimates of carrier phase float ambiguities will be attained sooner, thus reducing the initial convergence period of PPP. Given the problem, this study seeks to improve mitigation of the pseudorange errors. The well-known multipath linear combination is used in two distinct ways: (1) to directly correct the raw pseudorange observables and (2) to stochastically de-weight the pseudorange observables. The improvements in the solution were calculated with respect to the conventional GPS PPP float solution, where the raw pseudorange observables were not modified or stochastically de-weighted. Corrections to the observables were made using the multipath linear combination from data obtained from the previous and same day. Minimal improvements were noted using the multipath observable from the previous day. Using the multipath observable from the same day was possible in real-time and post-processing modes, showing an improvement in the rate of convergence for 48 and 57 % of the data, respectively. An improvement in the rate of convergence for 34 % of the data was observed when the pseudorange measurements were stochastically de-weighted using the multipath observable. Datasets with no improvements from directly correcting the raw pseudorange observables (43 %) or stochastically de-weighting the pseudorange observables (66 %) presented similar quality of results as the conventional PPP solution.

Keywords GPS · Precise point positioning · Convergence · Pseudorange multipath · Pseudorange noise · PPP

G. Seepersad (✉) · S. Bisnath
York University, Toronto, ON M3J 1P2, Canada
e-mail: GSeeper@yorku.ca

S. Bisnath
e-mail: SBisnath@yorku.ca

Introduction

PPP is a popular technique to process data from GPS receivers by introducing precise satellite orbit and clock information. Typically, a dual-frequency GPS receiver is utilized, with the dual-frequency pseudorange and carrier phase measurements linearly combined to remove the first-order effect of ionospheric refraction. The tropospheric refraction is also estimated along with the position, receiver clock error and real-valued carrier phase ambiguity parameters from the measurements (Héroux et al. 2004; Kouba and Héroux 2001; Zumberge et al. 1997).

PPP is considered a cost-effective technique as it enables static, sub-centimeter horizontal and few centimeter vertical positioning with a single GPS receiver, in contrast to methods such as relative GPS, RTK and Network RTK which require multiple receivers. PPP can be used for processing of static and kinematic data, both in real time and post-processing (Bisnath and Gao 2008; Ge et al. 2008; Geng et al. 2010; Héroux et al. 2004; Laurichesse et al. 2009).

PPP requires a relatively long initialization period, few tens of minutes at least, for the carrier phase ambiguities to converge to stable values and for the position solution to reach its optimal precision. This situation is primarily caused by the estimation of the carrier phase ambiguities from the relatively noisy pseudoranges. The result is that

Published online: 01 August 2014

PPP can take full advantage of the precise but ambiguous carrier phase observations; however, the length of time it takes to reach the optimal solution is a major disadvantage to the wider use of the technique. If, for example, the pseudoranges were more precise, then there would be a reduction in the convergence period.

Within PPP research, there has been a lack of attention given to the mitigation of pseudorange multipath and noise. Currently, the primary research avenues to reduce initial convergence focus on ambiguity resolution and processing of multi-GNSS constellations. With ambiguity resolution, Collins (2008) saw improvements in hourly position estimates by 2 cm and Geng et al. (2010) saw noticeable hourly improvements from 1.5, 3.8 and 2.8 to 0.5, 0.5, 1.4 cm for north, east and up, respectively. With the use of the modernized GPS, GALILEO, Beidou and GLONASS, there are several advantages to be gained which include more visible satellites, greater signal power level and more potential observable combinations, potentially resulting in improved positioning accuracy, availability and reliability (Shen and Gao 2006). According to Li and Zhang (2013) by including GLONASS, the average convergence time of GPS + GLONASS PPP float solution was shortened by 45.9 % from 22.9 to 12.4 min in static mode and by 57.9 % from 40.6 to 17.7 min in kinematic mode, respectively. Pseudorange multipath and noise together represent the largest remaining unmanaged error source in PPP. The amplitude of the multipath-induced errors in carrier phase observations is limited to a quarter wavelength or about 5 cm, but is typically well below 2 cm. Pseudorange multipath can have a magnitude of up to 10–20 m as it depends directly on the distance to the reflector (Dixon 1991). Currently, Hatch filtering is being performed in the position domain of the PPP software used in this study to mitigate pseudorange multipath and noise with minimal improvements in the rate of convergence (Seepersad 2012). As a result, additional forms of pseudorange multipath and noise mitigation should be considered. This study seeks to address this shortcoming of the technique by the following approaches: (1) modeling pseudorange multipath and noise and reducing from the original observable, and (2) pseudorange multipath and noise-based stochastic modeling.

Multipath observable

The colored noise of the pseudorange consists of the multipath and noise, which may have been caused by multiple signal reflections around the satellite and receiver antenna, in cable connectors, and variations from instrumental delays, and possibly due to temperature variations which can occur at different levels: antenna, cables, amplifiers, splitters, receivers, etc. (Defraigne and Bruyninx 2007). To characterize the pseudorange multipath for each satellite, the so-called pseudorange multipath observable is computed (Hofmann-Wellenhof et al. 2001; Leick 2004). A linear combination of the pseudorange and carrier phase measurements is used. By convention, the carrier phase multipath and noise, approximately two orders of magnitude smaller than the pseudorange multipath and noise, are neglected in this calculation. The estimate of pseudorange multipath and noise on L_1 (mp_1) is presented in (1) and on L_2 (mp_2) in (2),

$$\mathrm{mp}_1 = P_1 - \left(1 + \frac{2}{\alpha - 1}\right)L_1 + \left(\frac{2}{\alpha - 1} - 1\right)L_2 \tag{1}$$

$$\mathrm{mp}_2 = P_2 - \left(\frac{2\alpha}{\alpha - 1}\right)L_1 + \left(\frac{2\alpha}{\alpha - 1} - 1\right)L_2 \tag{2}$$

where P_1 is the measured pseudorange on L_1 (m), P_2 is the measured pseudorange on L_2 (m), f_1 is the L_1 frequency, and

$$\alpha = \left(\frac{f_1}{f_2}\right)^2 \tag{3}$$

with frequencies $f_1 = L_1$ frequency 1.5754 GHz and $f_2 = L_2$ frequency 1.2275 GHz.

This combination primarily contains pseudorange multipath and noise with no possible distinction between them, plus one constant component associated with phase ambiguities, and one component associated with instrumental delays.

Under the conditions that (1) multipath and noise have a zero mean during a period T_m, (2) the hardware delays are constant during T_m and (3) no cycle-slips occur during T_m. The multipath and noise can be obtained through (4) and (5) as,

$$\mathrm{MP1} = \mathrm{mp}_1 - \mathrm{mp}_{1T_\mathrm{m}} \tag{4}$$

$$\mathrm{MP2} = \mathrm{mp}_2 - \mathrm{mp}_{2T_\mathrm{m}} \tag{5}$$

where $\mathrm{mp}_{1T_\mathrm{m}}$ and $\mathrm{mp}_{2T_\mathrm{m}}$ are the average of mp_1 and mp_2, respectively, over the period T_m. The average is removed in order to eliminate the constant components. The quantity mp_1 and mp_2 contains the white noise components and multipath components with periods smaller than T_m (Defraigne and Bruyninx 2007). The $\mathrm{mp}_{1T_\mathrm{m}}$ and $\mathrm{mp}_{2T_\mathrm{m}}$ terms are dual-frequency carrier phase-biased combination, due to the inclusion of both L_1 and L_2 in the calculation of MP1 and MP2. The limitations on the use of this technique include: Multipath is not actually a zero mean phenomena, and the pseudorange multipath observable also includes the carrier phase multipath and noise.

Illustrated in Fig. 1 is the "multipath" estimate of the P_1 observable for PRN 22 at station ALGO (Algonquin, Canada) for DOY 183 of 2012 with a data rate of 30 s. The

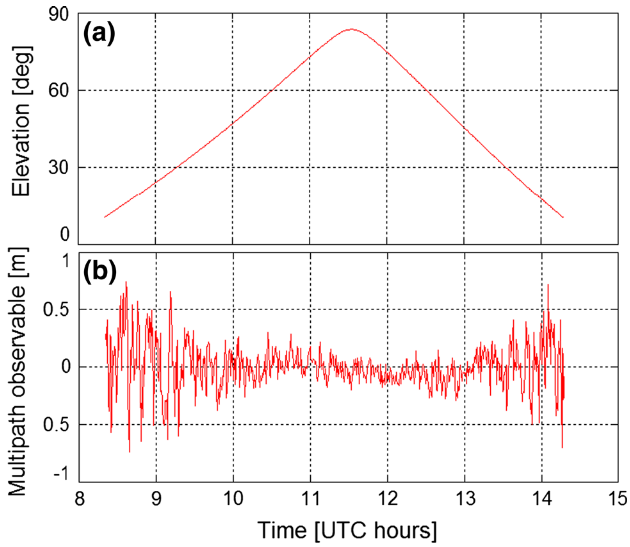

Fig. 1 Comparison of the elevation angle, sub-plot (**a**) and the ionospheric-free pseudorange multipath observable, sub-plot (**b**), for PRN 22 at ALGO on DOY 183 of 2012

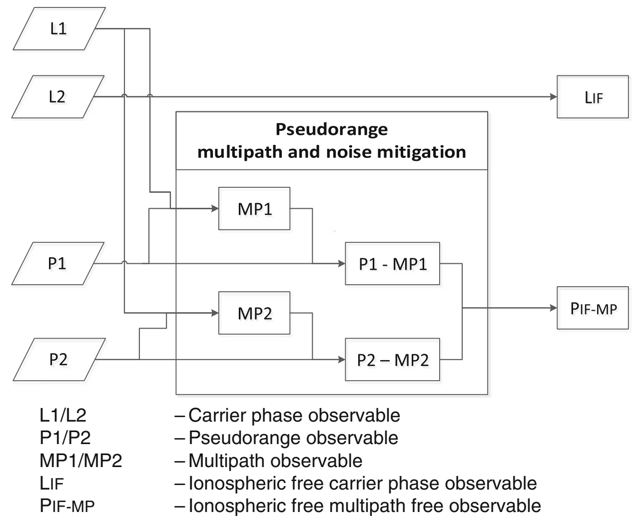

Fig. 2 Measurement processing flow augmented by multipath mitigation modules

site ALGO was selected as it showed typical ground bounce multipath, which was present at most of the data of the sites processed. The multipath time series for these data has a standard deviation of 28 cm and illustrates the characteristics of typical ground bounce multipath observed with a geodetic GNSS antenna, as at lower elevation angles there is higher multipath and as the observed elevation of the satellite increases, the multipath decreases.

Implementation of pseudorange mitigation using multipath observable

Conventional float PPP software requires dual-frequency measurements to calculate the ionospheric-free pseudorange and carrier phase observables. Illustrated in Fig. 2 is the measurement processing flow present in conventional PPP software augmented with the multipath mitigation module. The module was designed to function under three different modes of operation: (1) the multipath observable generated from the previous day (real time), (2) the multipath observable generated from the same day (post-processing) and (3) the multipath observable generated in real time using a running average (real time). The first step in the module is to obtain the required multipath observable depending on the user-defined mode of operation. The modes of operation consist of generating the multipath observable from the previous day or within the same day. The multipath observable generated from the previous day is available in real time, and the multipath observable generated within the same day has the functionality of being applied in real time or during post-processing. This step is followed by the correction of the raw P_1 and P_2 measurements by using the respective MP1 and MP2 observables. The final phase is the ionospheric linear combination of the corrected P_1 and P_2 and the L_1 and L_2 observables to give P_{IF} and L_{IF}, respectively.

Dataset, processor and processing parameters for this study

To examine the utility of the proposed error mitigation approaches, GPS data from 300 IGS stations observed from DOY 183 to 189 in 2012 with a data rate of 30 s were processed using the York-PPP software. York-PPP was developed based on the processing engine used by the online CSRS-PPP service. The sites chosen were a subset of those processed regularly by most IGS Analysis Centres, representing a good global distribution as illustrated in Fig. 3. Dual-frequency receivers tracking either the C/A or P(Y)—code on L_1—were used. For receivers that do not record the P_1 observable, the P1C1 code bias correction was applied. Settings used for the evaluation include the ionosphere-free combination of L_1 and L_2 data, 2 m and 15 mm a priori standard deviations for ionosphere-free pseudorange and carrier phase observations, respectively, and a 10° elevation cut-off angle. IGS final 5 min orbit and 30 s clock products were used. The data from the IGS stations were processed in static mode. Receiver clocks were estimated epoch by epoch. The zenith tropospheric delays were estimated every 60 min with a priori standard deviation of 2 cm/sqrt (hour). The station coordinates were estimated with an initial constraint of 1 km.

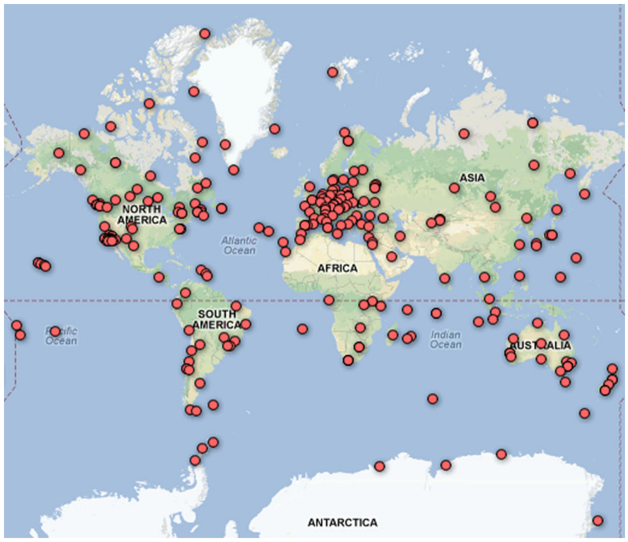

Fig. 3 Global distribution of the selected 300 IGS stations

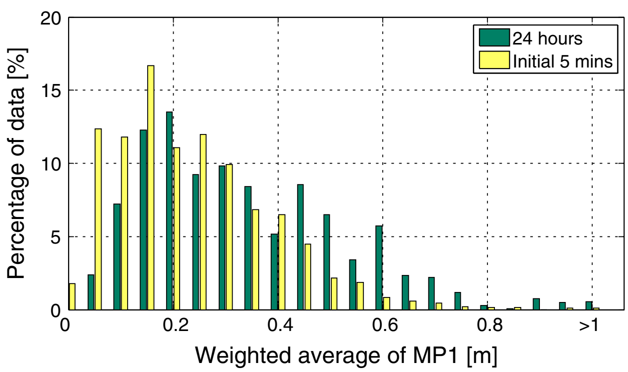

Fig. 4 Histogram illustrating the distribution of the MP1 rms for 24-h data arc and initial 5 min generated by TEQC for each dataset from 300 sites for DOY 183–189 of 2012

To characterize the magnitude of pseudorange multipath and noise present, the TEQC software (Estey and Meertens 1999) was used to generate the MP1 rms for each dataset processed for the entire 24-h data arc and initial 5 min. Presented in Fig. 4 is a histogram illustrating the distribution of the MP1 rms. The entire 24-h data arc was used to reflect the quality of multipath at the site and initial 5 min period to reflect the quality of the pseudorange measurements used to initialize the carrier phase ambiguity component. The MP1 rms represents a weighted average of the pseudorange multipath and noise grouped by elevation angle bin sizes of 5° and weighted by the number of observations present within each bin. The average MP1 rms for the 24 h data arc was 34 cm with a standard deviation of 20 cm, while the initial 5 min period was 23 cm on average with a standard deviation of 15 cm indicating that on average, during initial convergence the pseudorange measurements were not as noisy in contrast to the entire 24-h data arc.

Pseudorange multipath and noise correction for PPP modeling

The methods presented are novel applications to PPP of existing methods to mitigate pseudorange multipath and noise. The following sections discuss each of the methods applied and quantify the reduction of the pseudorange multipath and noise and the reduction of the PPP initial convergence period.

A receiver in static mode, in an unchanged user environment, would have a daily repeatable multipath observable if the so-called sidereal shift is removed. With the sidereal shift removed, the pseudorange multipath to be corrected for in real time as multipath is a function of the satellite-receiver geometry. The sidereal shift represents the difference between the sidereal and solar day, as the GPS satellites appear in their positions approximately 4 min (236 s) earlier each day (Agnew and Larson 2007). To graphically illustrate this phenomena, PRN 22 multipath observable estimate at the site ALGO was selected as the initial satellite arc ranged from 30° to 10° (setting), as shown in Fig. 1. The sidereal shift was applied to align the multipath observable for DOY 183 and 184 as illustrated in Fig. 5. A sidereal shift of 247.65 s was applied. The limitation of this shift is due to the observation rate of 30 s; when the shift is applied, the observations do not exactly align. With the shift applied, the corresponding epoch on DOY 183 is 8 s earlier than the nearest epoch on DOY 184. In Fig. 5, the correlation between DOY 183 and DOY 184 is clearly visible, as the peaks and valleys correspond.

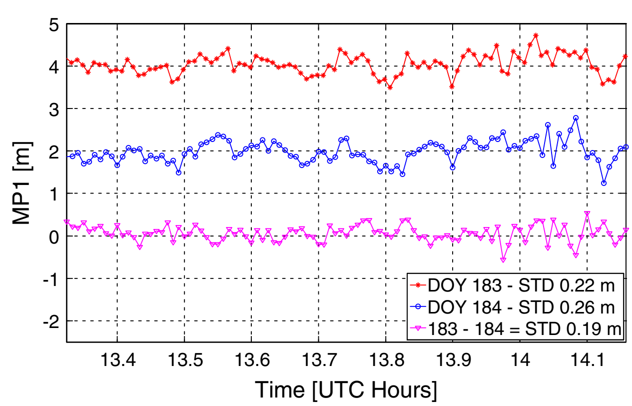

Fig. 5 Comparing the pseudorange multipath observable for PRN 22 at ALGO, for DOY 183 and 184 of 2012 in elevation range of 10°–30°. The vertical offsets 4 m for DOY 183 and 2 m for DOY 184 were applied to each time series for illustration purposes

As a result of the multipath observable not being accurately aligned between DOY 183 and 184, as the observations files have a sampling rate of 15 or 30 s, minimal improvements were seen. The average sidereal lag for GPS week 1695 is 246 s. Satellite PRN 22 on DOY 183, with the sidereal shift applied, was still approximately 7 s from the nearest node. To overcome this limitation, the possible benefits of interpolating the multipath observable from the previous day were examined. The interpolated multipath observable was simulated using MATLAB's linear interpolated function INTERP1. Minimal improvements were noted. Interpolating the time series from DOY 183 and subtracting each corresponding node from DOY 184 reduced the standard deviation of the differences from 0.19 to 0.17 m. A 2 cm improvement in the standard deviation of the pseudorange is not significant to improve the quality of the signal to reduce convergence in PPP (Seepersad 2012). Also, aliasing of the multipath frequencies is another limitation of why the multipath observable from DOY 183 cannot be used to effectively mitigate the multipath from DOY 184. Illustrated in Fig. 5 between UTC hours 14 and 14.1 multipath observable is aliased by the 30 s data rate making it challenging to interpolate through such a poorly sampled data profile.

Also, examined is using the multipath observable from within the same day, which is only possible through post-processing of the data, as the ambiguity component is eliminated by finding the average of the entire data arc. This method would be the most effective as it accurately represents the pseudorange multipath and noise present within the data. In PPP, the ionospheric linear combination is used, which triples the measurement noise versus the noise on L_1 or L_2 (Leandro 2009). This magnification indicates why the multipath observable generated within the same day would cause a significant reduction in the convergence time of PPP in contrast to the multipath observable from the previous day. In some cases, the noise may not be entirely eliminated as the ambiguity component may not have been accurately removed, as well as biases which may have been introduced.

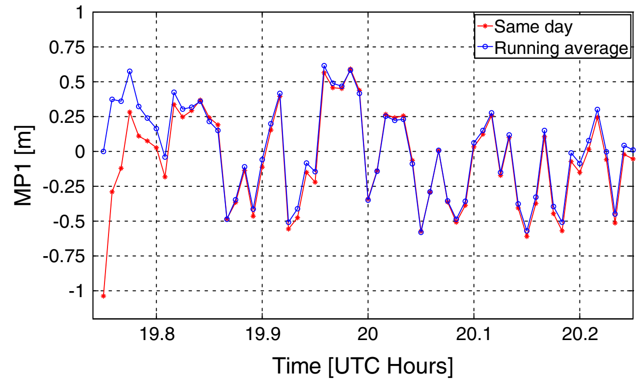

Fig. 6 Real-time multipath observable (running average) with poor initialization compared to post-processed multipath observable (average) for ALGO PRN 28

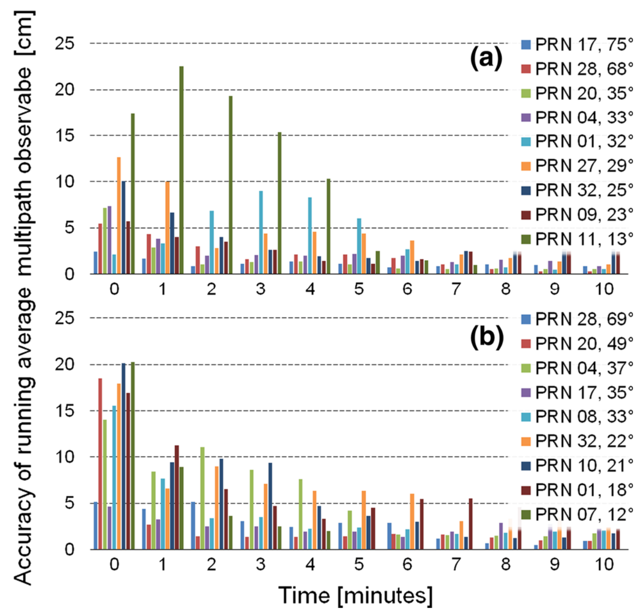

Fig. 7 Sites ALGO sub-plot (**a**) and AMBF sub-plot (**b**) for DOY 184 of 2012, illustrating the accuracy of the running average multipath observable using different bins of data to initialize the solution

Real-time correction

The running average is a simple recursive algorithm to estimate the $\mathrm{mp}_{1T_\mathrm{m}}$ and $\mathrm{mp}_{2T_\mathrm{m}}$ terms. The running average calculation of the ambiguity component is precise, but requires several hours of data to obtain an equivalent level of accuracy as the same day multipath observable because of the ambiguity component present in this observable. The real-time multipath observable generated as the data are collected illustrates a high level of precision but low accuracy due to the bias present. This effect is attributed to poor initialization due to a high variation in the pseudorange multipath and noise (same problem in range domain as for PPP in position domain). Another limitation is no corrections are applied during initialization of the running average. Presented in Fig. 6 is a 1.1 m difference between the same day average and the running average during initialization. In Seepersad (2012), few improvements were seen using the running average as a result of this convergence period. To improve the efficiency of the running average, the advantages of initialization using additional data were examined.

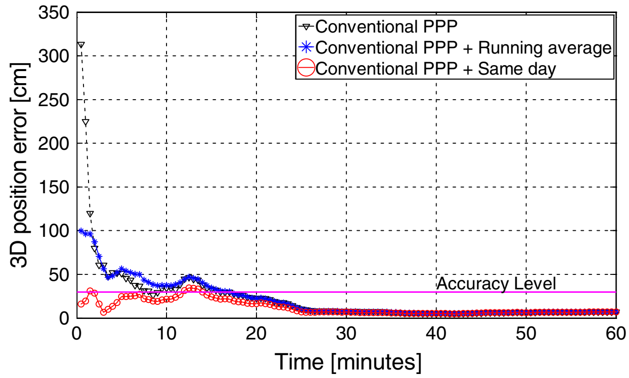

Fig. 8 Site NVSK for DOY 183 of 2012 with an initial MP1 rms value of 36 cm, illustrating improvements in initialization using the running average and instantaneous convergence using the same day multipath observable

In Figs. 7 and 8, the different time bins for initializing the running average are examined at the sites ALGO and ABMF on DOY 184 of 2012. Measurements for each satellite present at the start of the dataset were binned with 1 min intervals with the maximum bin size of 10 min. To quantify accuracy, the initialized running average was compared to the same day multipath observable.

Figure 7 illustrates the rms error of each of the initial 9 satellites present for different initialization periods for the sites ALGO sub-plot (a) and AMBF sub-plot (b). As expected, satellites at higher elevation angle initialized more accurately due to less ground bounce multipath and noise. At the site ALGO, all satellites except PRNs 17 and 28 had an initial elevation angle of less than 30°. The higher accuracy for PRNs 04, 09, 20 and 32 is due to low multipath and noise present during initialization allowing for accurate estimation and removal of the ambiguity component present in each multipath observable. For PRN 11 with an initial elevation angle of ~13°, the solution had an initial rms error of 18 cm, and after increasing the bin size to 5 min, the accuracy of the multipath observable became comparable to that of the other satellites. It is noted for PRN 01 that as the bin size was increased from 0 to 5 min, the accuracy of the running average deteriorated from 2 to 6 cm. The deterioration was as a result of spikes at minute 2 and 3 in multipath observable due most likely to ground bounce multipath.

During initialization at the site ABMF (Les Abymes, Guadeloupe), all satellites had a noticeably higher rms error when compared to the satellites observed at site ALGO. The larger rms may have been due to the local environment of the receiver being more prone to higher levels of pseudorange multipath and noise. PRNs 32, 10, 07 and 01 had an elevation angle of less than 30°. PRN 17 and 28 initialized accurately. A linear trend is noted, similar to that presented at the site ALGO, as more data were used during initialization, the accuracy of the running average improved.

The benefits of initialization are presented in Fig. 7, which shows the reduction of the magnitude of the rms error when different bin sizes were used. It is recommended that 20 epochs (10 min at 30 s data rate) be used to initialize the multipath observable.

Application of correction techniques

To illustrate the improvements of the running average and same day multipath observable, the site NVSK (Novosibirsk, Russia) on DOY 183 for the study cases conventional PPP, multipath observable used from the same day and with a running average, illustrated in Fig. 8. A loose convergence threshold of 30 cm 3D position error was set to examine the time the solution took to converge. The conventional and running average PPP solution converged in 17 min, while the solution using the multipath observable from the same day instantaneously converged. While the running average multipath observable did not improve convergence, improvements were seen at the start of initialization from 313 to 100 cm. In the context of stability, the rms error of the first 10 min was analyzed. Conventional PPP had an rms error of 100 cm. When the pseudorange and multipath noise were corrected using the running average and same day technique, the rms error was reduced to 60 and 21, cm, respectively.

Data of all 300 sites were processed for each of the study cases for DOY 183–189 of 2012 for a total of 2,010 datasets. A 30 cm 3D accuracy threshold was set to examine the time the solutions took to converge. The results are presented in Fig. 9. The most critical period for

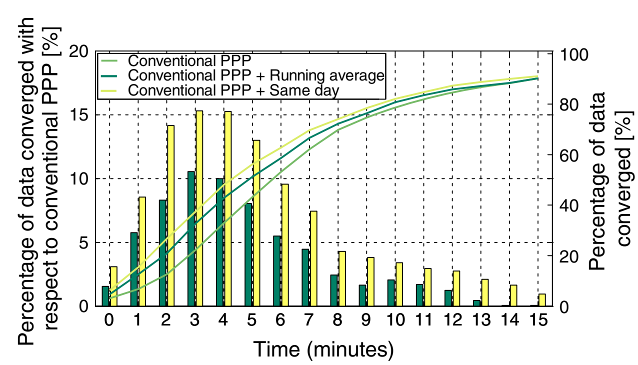

Fig. 9 Percentage improvement with respect to conventional PPP for each pseudorange multipath and noise mitigation technique. The *line graph* illustrates the percentage of the data that converges to a 30 cm 3D accuracy level for each of the three study cases. The *bar chart* illustrates the improvements using the running and same day average with respect to the conventional PPP solution

convergence is within the first 20–30 min when the carrier phase measurements begin to take over the solution. The most significant improvements were noted within the initial 15 min, which shall serve as the focus of the analysis.

Figure 9 quantifies the improvements of using the pseudorange multipath and noise observable to mitigate the raw P_1 and P_2 observables. The line graph illustrates the percentage of the data that converges to meet a 30 cm 3D accuracy level for each of the three study cases. The bar chart illustrates the improvements using the running and same day average with respect to the conventional PPP solution. A plateau was achieved after 15 min with a gentle linear trend noted from 15 to 60 min after which 100 % of the data had converged. After 15 min of data processing, 90 % of the data achieves a 30 cm 3D accuracy level. The 10 % of the data that did not converge within the first 15 min needed additional time (ranging from few to 10s of minutes) with little improvement in convergence time regardless of the mitigation technique applied.

Post-processed pseudorange multipath and noise correction

This method is possible by post-processing the dataset, generating the multipath observable that is fed into the PPP processor. Significant improvement in the rate of convergence was noted as a result of the real-valued ambiguity component, which is accurately removed, and the multipath observable is generated from the entire dataset accurately representing the pseudorange multipath and noise present. The multipath observable provides corrections during the first epoch, thus improving the initial coordinates which is critical for reducing convergence period in PPP. The noise on the pseudorange observable is one of the primary reasons for the current convergence period within the conventional PPP solution. Improvements of 3, 9, 14, 15 and 15 % were seen in contrast to the conventional PPP within the initial 5 time bins.

Real-time pseudorange multipath and noise correction

The less effective of the two methods was the running average. Previous work (Seepersad 2012) showed the running average producing similar results as the conventional PPP. This was expected, as both the conventional PPP solution and the running average have a convergence period due to the required estimation of the ambiguity parameter. The improved method presented uses the initial 10 min to initialize the recursive estimator of the ambiguity component present in the multipath observable. An improvement was noted in convergence when the running average used a 5 min data bin to initialize. Improvements

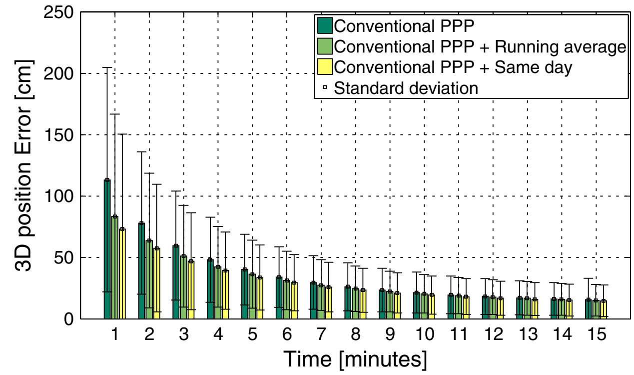

Fig. 10 3D mean and standard deviation illustrating improvements in position estimation for each study case used to mitigate pseudorange signal

of 2, 6, 8 and 11 % were seen in contrast to the conventional PPP within the initial 5 min time bins.

Figure 10 examines the average quality of all 2,010 datasets each minute for the first 15 min. The bars represent the average error, and the error bars represent the standard deviation of the error. The convergence trends are as expected with the largest errors present during initialization, and the quality of the solution improves exponentially with time. The conventional PPP solution initialized with an average error of 113 ± 91 cm. Using the running and same day average, the error reduced to 83 ± 84 and 73 ± 77 cm, respectively. After 15 min of processing, the errors for the conventional PPP, running and same day average reduced to 15 ± 17, 15 ± 13 and 15 ± 13 cm, respectively. With the conventional PPP technique, at the 15th minute, the average error reduces but the standard deviation increases by 4 cm. This unsettling period is typical of conventional PPP during initial convergence. Regardless of which pseudorange multipath and noise mitigation technique was applied, the unsettling period was reduced or eliminated. It is postulated that the reduction or elimination of the unsettling period resulted from the more precise pseudorange range signal being used to initialize the carrier phase ambiguity component.

Pseudorange multipath and noise stochastic modeling for PPP

The following method has been proposed to take advantage of the precise but biased nature of the running average. Typically, if a stochastic model is used at all, it typically relies on the tracked satellite's elevation angle with respect to the receiver. The use of elevation angle-based weighting is very approximate, and its use may produce reduced-accuracy positioning results. The relationships between the

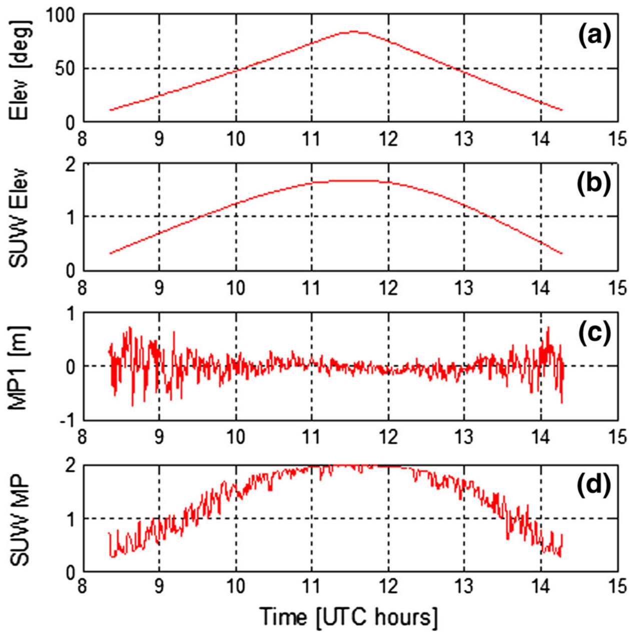

Fig. 11 Comparison of stochastic de-weighting functions of pseudorange observables collected from PRN 22 from ALGO DOY 183 of 2012. Sub-plot **a**, **c** illustrates the elevation angle and multipath observable. Sub-plot **b**, **d** illustrates the sigma of unit weight for the elevation angle and multipath observable

observable and other weighting criteria such as the satellite elevation angle are also analyzed.

Conceptually, in stochastic de-weighting using the multipath observable, the multipath constituent in the pseudorange functional model is not treated as a deterministic quantity to be estimated, but rather it is coupled with the receiver thermal noise and tracking error components, and its variance is estimated. The strength of this model is that it allows for real-time compensation of the effects of the pseudorange multipath and noise in the stochastic model, as long as realistic stochastic models are applied for each epoch in the position estimation process (Bisnath and Langley 2001). The variance is calculated over a bin size of 5 epochs. The hyperbolic function is used to normalize the weights where 100 represents the smoothing parameter. The stochastic weights for the pseudorange observables (SUW_MP) were calculated by finding an average of $\mathrm{SUW\_MP}_1$ and $\mathrm{SUW\_MP}_2$, where

$$\mathrm{SUW\_MP}_{1|2} = \left(\left(\tanh\left(\mathrm{weightsMP}_{1|2}/100\right)\right)\right) + \mathrm{sine}(\mathrm{elevation}) \quad (5)$$

Presented in Fig. 11 are the data obtained from ALGO, DOY 183 for PRN 22. Figure 11a, c illustrates the elevation angle and multipath observable with respect to the time of observation, and the respective sigma of unit weight illustrated in Fig. 11b, d. As expected, the weight derived from the elevation angle of the satellite is a simple

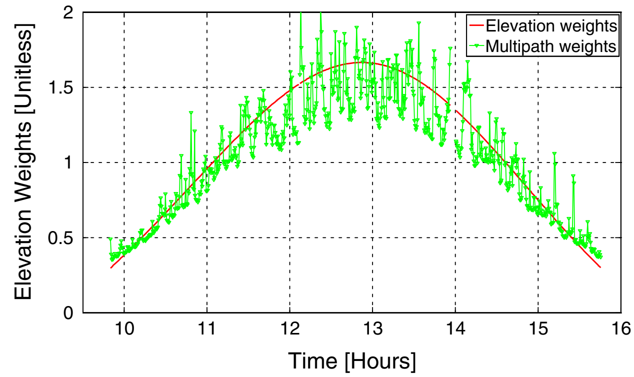

Fig. 12 Stochastic de-weighting used for the pseudorange measurement for PRN 22, DOY 183 of 2012 from the site ALGO

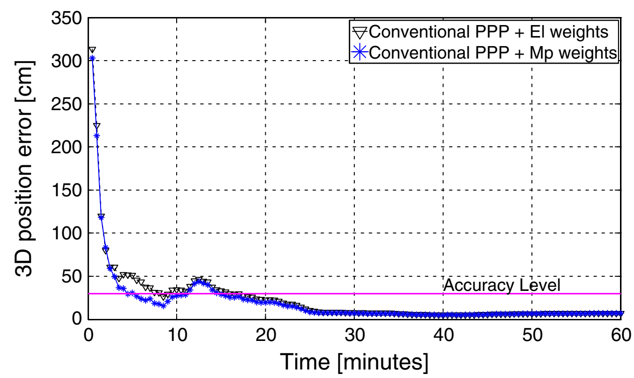

Fig. 13 Site NVSK for DOY 183 of 2012 with an initial MP1 rms of 36 cm, illustrating momentary convergence within the first 10 min and then re-convergence and a steady state being attained within 16 min

weighted function, while the weight derived from the multipath observable does reflects the measurement precision, which is a function of the pseudorange multipath and noise.

Presented in Fig. 12 is an example of the elevation and multipath stochastic de-weighting used for the pseudorange measurement. This was used for PRN 22, DOY 183 from the site ALGO. Illustrated are the advantages of using the multipath stochastic de-weighting scheme as in real time takes into effect the pseudorange multipath and noise in the stochastic model.

At the site NVSK for the DOY 183, the study cases elevation weights and multipath weights were examined. Similarly, a 3D accuracy threshold of 30 cm was set, examining the convergence time of the solution, illustrated in Fig. 13. When elevation weights were applied, the initial 3D error was 314 cm; with the multipath weighting scheme applied, the 3D error was reduced to 302 cm. While the improvements during initialization was minimal, the solution consistently remained more accurate for the first

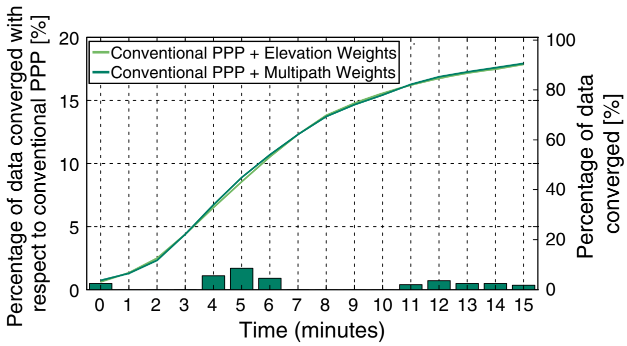

Fig. 14 Percentage improvement with respect to conventional PPP for each stochastic de-weighting scheme. The *line graph* illustrates the percentage of the data that converges to a 30 cm 3D accuracy level for each study case. The *bar chart* illustrates the improvements using the proposed multipath de-weighting scheme with respect to the elevation de-weighting scheme

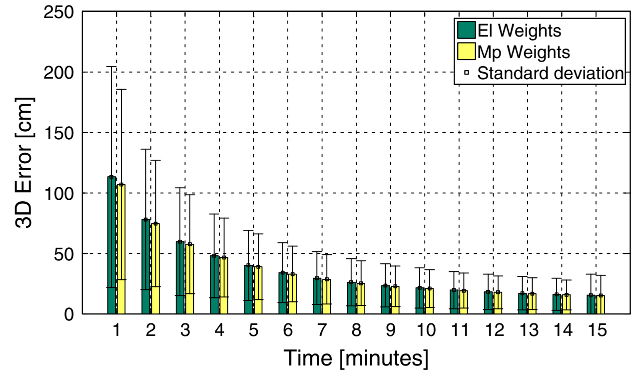

Fig. 15 3D mean and standard deviation illustrating improvements in position estimation for each stochastic de-weighting scheme

30 min at which few millimeter differences existed. Presented in this dataset is one of the challenges in defining when convergence is actually attained. Initially, the study case using multipath weights converged in 4.5 min, while using the elevation weights converged in 8 min. The solution enters an unsettling period, during time period of 9–16 min when elevation weights were used and 11–14.5 min when multipath weights used. In the context of stability, the rms error of the first 10 min was analyzed. Using elevation weights, the solution had an rms error of 100 cm and with multipath weights 92 cm representing an 8 cm reduction in instability.

To examine the quality of the improvements on convergence, the stochastic de-weighting scheme using the multipath observable was compared to the conventional PPP which uses elevation weights, as illustrated in Fig. 14. Similarly, the first 15 min is used to examine improvements in initialization and convergence time for the study cases multipath and elevations weights. The line graph illustrates the percentage of the data that converges to meet a 30 cm 3D accuracy level for each study cases. The bar chart illustrates the improvements of using the multipath weights with respect to conventional PPP, which uses elevation weights. The bar graph illustrates time periods where improvements were typically seen. These can be grouped in three time periods, during initialization, 4–6 and 11–15 min. These three periods represent when the multipath weighting scheme improves the rate of convergence. During initialization, the solution is most sensitive as it is a single point positioning solution. Within 4–6 and 11–15 min time periods, most solutions were in the unsettling period and the multipath weight aids the solution stability.

Figure 15 examines the overall quality of the solution each minute for the first 15 min. The bars represent the average error of all datasets processed, and the error bars represent the standard deviation of the error. The convergence trends are as expected with the largest errors present during initialization and the quality of the solution improving exponentially with time. The elevation weights initialized with an average error of 113 ± 91 cm. Using the multipath weighting scheme, the error reduced to 107 ± 79 cm. After 15 min of processing, the errors for the elevation and multipath weights reduced to 16 ± 17 and 16 ± 17 cm, respectively. For both elevation and multipath weights at the 15th minute, the average error is reduced but the standard deviation increases by 4 and 3 cm, respectively. This unsettling period is typical of conventional PPP during initial convergence. When either of the pseudorange multipath and noise mitigation techniques were applied, the unsettling period was significantly reduced or eliminated.

Conclusions and recommendations

Pseudorange multipath and noise are the largest remaining unmanaged error sources in PPP. It is proposed that by reducing the effects of the multipath and noise on the pseudorange observable, carrier phase ambiguities will reach a steady state at an earlier time, thus reducing the initial convergence and re-convergence period of PPP. The multipath linear combination was calculated and used to mitigate the raw pseudorange observable based on the magnitude of the pseudorange multipath and noise present. To correct the raw observables, two different methods were applied: (1) running average and (2) the same day multipath observable. The multipath observable from the previous day was not included in this study as previous work showed minimal improvements to initialization and convergence time.

Table 1 Summary of examined methods to mitigate pseudorange multipath and noise by correcting the raw observables

Raw pseudorange correction	Same day	Running averaging
Multipath	Yes	Yes
Noise	Yes	Yes
Real time	No	Yes
Extra data required	Yes	No
Complexity	High	Medium
Limitations	Post-processing required	Filter has a convergence period
% datasets improved	57	48

Table 2 Summary of examined methods to mitigate pseudorange multipath and noise by stochastically de-weighting observables

Stochastic de-weighting	Multipath weighting	Elevation weighting
Multipath	Yes	No
Noise	Yes	No
Real time	Yes	Yes
Extra data required	No	No
Complexity	Medium	Low
Limitations	Increased complexity	Too general
% datasets improved	34	–

GPS data from 300 IGS stations observed during 1 week (DOY 183–189) in 2012 were used to examine the utility of the proposed error mitigation approaches for improvements in convergence of the estimated York-PPP float solution. The multipath observable from within the same day was used to correct the raw pseudorange. This method is possible by post-processing the dataset, generating the multipath observable which is fed into the PPP processor. The improved precision of the pseudorange measurements allowed for a faster initial convergence period. Fifty-seven percent of the data converged faster to meet the 30 cm threshold when the same day filter was used in contrast to the conventional PPP solution. This method was most effective as it allowed the ambiguity component to be accurately removed and therefore accurately removed the pseudorange multipath and noise from the pseudorange measurements.

The running average filters the pseudorange for multipath and noise in real time. Its major limitation is the requirement of several epochs of data to successfully average the ambiguity, by using a simple recursive algorithm to estimate the ambiguity component and filter the pseudorange observables. An initial 10 min of data was used to initialize the running average resulting in 48 % of the data to converge faster (Table 1).

To utilize the precise but biased nature of the running average, a pseudorange multipath and noise stochastic de-weighting scheme was designed. The benefits of either de-weighting using the elevation angle or the multipath observable were observed when compared to the conventional PPP solution, which used equal weights for all the pseudorange measurements. A 3D accuracy level of 30 cm was set to examine the improvements of both methods over the conventional PPP solution. Overall improvements of 34 % were observed over conventional PPP when using the multipath observable (Table 2).

Of all the methods presented, the stochastic de-weighting using the running average multipath observable is recommended to become a component of the conventional PPP processor. The strength of this model is that it allows for real-time compensation of the effects of the pseudorange multipath and noise in the stochastic model, as long as realistic stochastic models are applied for each epoch in the position estimation process. Limitations of the stochastic de-weighting model include the computational load in contrast to the technique currently used and the binning of the data.

Integer ambiguity resolution of undifferenced carrier phase observables has been a difficult task in GPS processing and even more troublesome in PPP, where undifferenced carrier phase is used. Future work would consist of augmenting pseudorange multipath and noise mitigation with ambiguity resolution. It is anticipated to see the ambiguity component to be resolved faster resulting in improved convergence period and solution accuracy.

Acknowledgments This research was funded by the Natural Sciences and Engineering Research Council of Canada. The results presented are derived from data and products provided by the International GNSS Service. The original PPP source code was provided by Natural Resources Canada.

References

Agnew DC, Larson KM (2007) Finding the repeat times of the GPS constellation. GPS Solut 11(1):71–76

Bisnath S, Gao Y (2008) Current state of precise point positioning and future prospects and limitations. In: International Association of Geodesy Symposia—observing our changing earth, vol 133, pp 615–623

Bisnath S, Langley R (2001) Pseudorange multipath mitigation by means of multipath monitoring and de-weighting. In: Proceedings of the international symposium on kinematic systems in geodesy, geomatics and navigation, Banff, AB, June, pp 392–400

Collins P (2008) Isolating and estimating undifferenced GPS integer ambiguities. In: Proceedings of ION-NTM-2008, Institute of Navigation, San Diego, CA, Nov, pp 720–732

Defraigne P, Bruyninx C (2007) On the link between GPS pseudorange noise and day-boundary discontinuities in geodetic time transfer solutions. GPS Solut 11(4):239–249

Dixon T (1991) An introduction to the global positioning system and some geological applications. Rev Geophys 29(2):249–276

Estey LH, Meertens CM (1999) TEQC: the multi-purpose toolkit for GPS/GLONASS data. GPS Solut 3(1):42–49

Ge M, Gendt G, Rothacher M, Shi C, Liu J (2008) Resolution of GPS carrier-phase ambiguities in precise point positioning (PPP) with daily observations. J Geodesy 82(7):389–399

Geng J, Meng X, Dodson AH, Teferle FN (2010) Integer ambiguity resolution in precise point positioning: method comparison. J Geodesy 84(9):569–581

Héroux P, Gao Y, Kouba J, Lahaye F, Mireault Y, Collins P, Macleod K, Tetreault P, Chen K (2004) Products and applications for precise point positioning—moving towards real-time. In: Proceedings of ION-GNSS-2004, Institute of Navigation, Long Beach, CA, Sept, pp 1832–1843

Hofmann-Wellenhof B, Lichtenegger H, Collins J (2001) GPS theory and practice, 5th edn. Springer, New York

Kouba J, Héroux P (2001) Precise point positioning using IGS orbit and clock products. GPS Solut 5(2):12–28

Laurichesse D, Mercier F, Berthias JP, Broca P, Cerri L (2009) Integer ambiguity resolution on undifferenced GPS phase measurements and its application to PPP and satellite precise orbit determination. J Inst Navig 56(2):135–149

Leandro RF (2009) Precise point positioning with GPS: a new approach for positioning, atmospheric studies, and signal analysis. PhD dissertation, University of New Brunswick, Canada

Leick A (2004) GPS satellite surveying, 3rd edn. Wiley, London

Li P, Zhang X (2013) Integrating GPS and GLONASS to accelerate convergence and initialization times of precise point positioning. GPS Solut. doi:10.1007/s10291-013-0345-5

Seepersad G (2012) Reduction of initial convergence period in GPS PPP data processing. MSc dissertation, York University, Toronto

Shen X, Gao Y (2006) Analyzing the impacts of Galileo and modernized GPS on precise point positioning. In: Proceedings of ION-NTM-2006, Institute of Navigation, Monterey, CA, Jan, pp 837–846

Zumberge J, Heflin M, Jefferson D, Watkins M, Webb F (1997) Precise point positioning for the efficient and robust analysis of GPS data from large networks. J Geophys Res 102(B3):5005–5017

Garrett Seepersad is a Ph.D. candidate at York University, Toronto, Canada, in the Department of Earth and Space Science and Engineering. He has completed his B.Sc. in Geomatics at the University of West Indies and his M.Sc. in Geomatics Engineering at York University. His area of research currently focuses on the development and testing of PPP functional, stochastic and error mitigation models.

Dr. Sunil Bisnath is an Associate Professor in the Department of Earth and Space Science and Engineering at York University in Toronto, Canada. His research interests include geodesy and precise GNSS positioning and navigation.